INVESTIGATIONS ON THE TURBULENCE BEHAVIORS OF THE CYLINDER WAKE WITH A NEW VOLUME PTV

Deog Hee Doh
Division of Mechanical & Information Engineering,
Korea Maritime University
1 Dongsam-dong, Yeongdo-gu, Busan, 606-791, Korea
doh@hhu.ac.kr

Gyeong Rae Cho
Division of Mechanical & Information Engineering,
Korea Maritime University
1 Dongsam-dong, Yeongdo-gu, Busan, 606-791, Korea
vpascal@paran.com

Hyo Jae Jo
Division of Naval Architecture & Ocean Engineering Systems,
Korea Maritime University
1 Dongsam-dong, Yeongdo-gu, Busan, 606-791, Korea
hjjo@hhu.ac.kr

ABSTRACT

Turbulence properties of a cylinder wake(d=10mm) have been investigated with a new volume PTV algorithm. The measurement system consists of of two-high-definition-cameras(1k x 1k), a Nd-Yag laser and a host computer.

A fitness function representing two-dimensional coherency has been adopted to sort out spurious vectors. A hybrid fitness function representing the relations between the fitness and the three-dimensional shortest distances constructed by the two collinears of the two cameras has been also adopted.

The constructed algorithm has been employed for the measurements of the cylinder wakes. The Reynolds numbers tested in this paper are 360, 540, 720, 900, 1080 and 1260. More than 10,000 instantaneous 3D vectors have been obtained by the constructed system. The volumetric distributions of the turbulence intensities (for u', v', w') indicates that clearly different patterns for all Reynolds numbers and implies that a regular pattern (like a similarity rule) for the turbulent properties exists.

INTRODUCTION

The accurate quantification of the turbulence properties in the near-wake region is of a priority interest concerning the physical analysis and the turbulence modeling of unsteady separated flows past bluff bodies. This comprehension is a prerequisite for elaborating adapted and efficient turbulent modeling techniques for this category of flows characterized by a double physical nature, organized and chaotic. In this context, the main objectives of the present study are to provide a detailed evaluation of the mean and fluctuating turbulent quantities in the near-wake field and in the vicinity of the wake region of a cylinder wake.

Monkewitz (1988) showed the existence of a local absolute instability in the wake at a Reynolds number of Re= 25. However Williamson (1996a) showed that a von Karman vortex street appears at a Reynolds number around 49. At a critical Reynolds number of Re=194 the wake flow becomes three-dimensional. The first three-dimensional instability that appears is the so-called "mode A instability" that is characterized by a spanwise wave-length of around 3D-4D, where D is the diameter of the cylinder. This mode is the result of an elliptic instability and it scales on the primary vortex core, which is the larger physical structure in the flow. Around Re=240 the instability changes from mode A to mode B. Mode B is characterized by a reduction in size of the spanwise wave-length by a factor of three. This instability scales on the braid shear layer which is the smaller physical structure of the flow (Williamson, 1996b; Thompson et al., 1996). In the subcritical range – for Reynolds numbers between Re=1000 and Re=200,000 – the flow in the vicinity of the cylinder is entirely laminar and transition happens somewhere in the free shear layer downstream of the cylinder. In this study, turbulence properties near the wake of a circular cylinder are investigated by using a newly constructed Volume PTV.

In the meantime, there have been many challengeable studies for obtaining spatial distributions of velocity vectors of the fluid flows. Arroyo and Greated (1991) and Kähler and Kompenhans (2000) showed the capability of the Stereo-PIV (SPIV) for probing three-dimensional properties of the flow fields. Hinsch (2002) and Chan et al.(2004) showed possibility of quantification of the complex flows by using Holography-PIV(HPIV). Digital-Holographic-PIV was firstly constructed by Coëtmellec et al.(2001). Very recently, Kim and Lee(2008) constructed in-line digital holographic PIV(DHPIV) by introducing a high-definition

camera (1K x 1K). Their results showed that the recovery ratio from the whole particles in the measurement volume was about 65% when the particle density was 25/mm³. This means that the whole identifiable particle numbers are about 8,500 among the 13,000 particles appeared in the measurement volume. Sung and Yoo(2001) introduced a phase-averaging PIV technique for obtaining three-dimensional wake structures of a circular cylinder wake by the use of 2D-PIV. They suggested to overcome the limits of the spatial resolution of the 3D-measurement techniques. Recently, a Tomographic PIV (Volume PIV) has been suggested by Scarano et al.(2006) and employed to the measurements of the cylinder wake.

The purpose of the study is to evaluate spatial distributions of the turbulent properties of a circular cylinder wake by using a newly constructed Volume PTV.

EXPERIMENTAL SET-UP

Fig. 3 shows the overall measurement system. A cylinder (D=10mm) was installed into a water channel(1100mm x 300mm x 300mm). Two digital cameras (Kodak ES1.0, 1k x 1k) were used for volumetric measurements and installed as seen in the figure. A Nd-Yag laser(120mJ, 15Hz) was used for flow visualizations. A logic controller (Labsmith, LC880) was used for synchronizations with the cameras and the Nd-Yag laser. In order to calculate the camera parameters a calibration plate on which the grid lines are installed with 4mm x 4mm distances. This plate was traversed in the measurement volume to the cameras' viewing direction). The Reynolds numbers tested were 360, 540, 720, 900, 1080 and 1260. The measurement volume was set to 60mm x 70mm x 20mm.
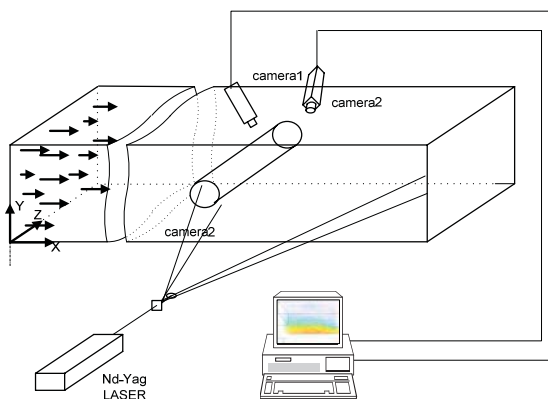

Fig. 1 Experimental set-up.

Principle of Volume PTV

The principle of the newly constructed volume PTV(particle tracking velocimetry) follows two steps. Firstly, camera calibration is carried out for the two cameras, through which the relations between the physical coordinate of the measurement volume and the photographical coordinate of the camera images is obtained. Next, finding

(tracking) process is made, in which the same particle pairs between the two time consecutive image frames.

Particle Image Matching. In order to attain three-dimensional measurement with two cameras, it is necessary to know their camera parameters. The 10-parameter method (Doh et al., 2002, 2004) was used to obtain them. In the 10-parameter method, 10 parameters (6 exterior parameters: $dis, \alpha, \beta, \gamma, m_x, m_y$, 4 interior parameters: c_x, c_y, k_1, k_2) are obtained. (α, β, γ) represents the tilting angles of the axes of the photographic coordinates against the absolute axes. The collinear equation for every point between the two coordinates is expressed as Eq. (1). c_x and c_y are the focal distances for x and y components of the coordinate. Δx and Δy are the lens distortions as expressed as Eq. (2).

$$x = c_x \frac{Y_m - m_x}{\sqrt{dis^2 - m_x^2 - m_y^2} - Z_m} + \Delta x$$
$$y = c_y \frac{Y_m - m_y}{\sqrt{dis^2 - m_x^2 - m_y^2} - Z_m} + \Delta y \tag{1}$$

$$\Delta x = (x/r) \times \left(k_1 r^2 + k_2 r^4\right),$$
$$\Delta y = (x/r) \times \left(k_1 r^2 + k_2 r^4\right),$$
$$r = \sqrt{x^2 + y^2} \tag{2}$$

$$F = c_x \frac{X_m - m_x}{\sqrt{dis^2 - m_x^2 - m_y^2} - Z_m} - (x - \Delta x) = 0 \quad,$$
$$G = c_y \frac{X_m - m_y}{\sqrt{dis^2 - m_x^2 - m_y^2} - Z_m} - (y - \Delta y) = 0 \tag{3}$$

The Eq. (2) can be converted to Eq. (3). Explanations on the symbols in the equations and the calculation process for the camera parameters are explained well in the reference (Doh et al., 2002).

Tracking Algorithm. Fig. 2 shows the tracking algorithm of the Volume PTV. Vector tracking algorithm is made as follows. (1) Obtain the 2-dimensional vectors for each camera within a certain displacement. Here, PM(particle movement) has been set to a certain pixel value according to the flow speed (Fig. 3). This procedure is called as time matching. (2) Find candidate of particle pairs on the image of camera 2. Here, Epipolar line has been used to find the candidate particles on the image of the camera 2. To save calculation time, a certain search area has been set as shown in Fig. 4. The particle pairs on this area are regarded as the candidates. For the particle 'n1' and 'n2', the same procedure for finding the candidates is made. Once the candidate (k2) of the particle image of the camera 2 for the initial point (k1) are found, the terminal point of the 2D vector is automatically decided since the 2D vectors had been already obtained. If the candidate for particle 'n1' is found within the Epipolar search area, the particle set of (k1,

n1, k2, n2) is sorted into the candidate group. (3) For the whole particles in the images of the camera 1 and the camera 2, the candidate group database is constructed. (4) For the candidate group database, a particle neighborhood value [PN] is set to a certain value [mm]. Within this PN, a vector fitness [VF] is calculated using Eq. (4). u_i represents the whole vectors within PN except the target vector itself and u_o represents the mean value of the whole vectors within PN except the target vector itself. (5) Lastly, a sigmoid-like hybrid fitness function is used for sorting out the most probable candidate from the candidate group database. Using PN and PM values implies to find a coherency of the neighborhood particles. It has been shown that the optimal parameters are PM=8 pixel, PN=5mm and VF=0.3.
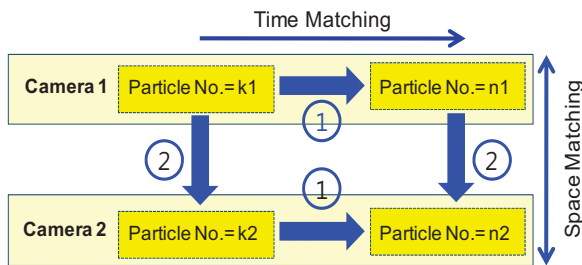
Fig. 2 Overall procedure for vector acquisitions.
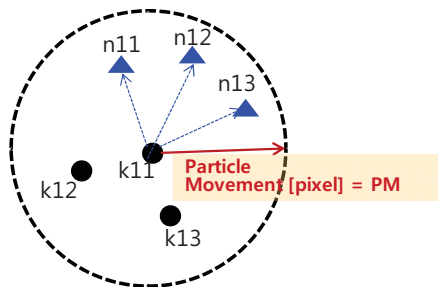
Fig. 3 Definition of particle movement [PM].
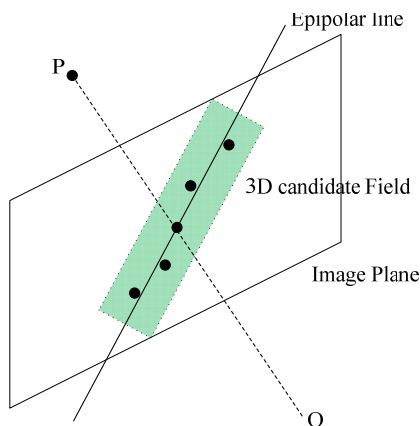
Fig. 4 Epipolar line and a search area.
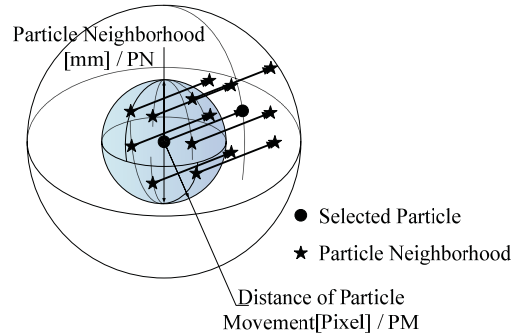
Fig. 5 Definition of particle neighborhood [PN].
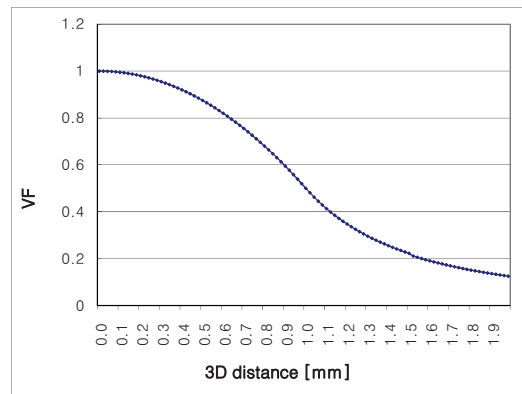
Fig. 6 Hybrid fitness function used for sorting the most probable candidate from the candidate group database.

$$Vector\ Fitness[VF] = \frac{\sum |u_i - u_o|}{\sum u_i} \tag{4}$$

$$f(x) = \begin{cases} -0.5x^2 + 1, & at \quad (0 \le x \le 1) \\ 0.5x^{-2}, & at \quad (x \ge 1) \end{cases} \tag{5}$$

RESULTS AND DISCUSSIONS

Fig. 7 shows the obtained instantaneous 3D vectors at Re=360. More than 10,000 vectors were obtained. This number is very meaningful because the number was recovered from the identified particles in one image. This implies that the vector recovery is almost close to 80~90% of the particles seen in the image. Fig. 8 show the obtained instantaneous 3D vector distributions interpolated onto 40 x 40 x 6 grids when the Reynolds number is 360.

Fig. 9 shows the turbulence properties of the wake at Re=360. w' component is bigger than u' and v' values. For all Reynolds number cases, $|w'| > |u'| > |v'|$ was satisfied, and each value was 2 times higher than others. w' distribution has a strong relation with that of the turbulent kinetic energy, which implies that w' component largely influences the turbulent properties of the wake.

Fig. 10 and Fig. 11 shows the $|u'|/U_o$ and $|v'|/U_o$ distribution, respectively for Reynolds 540, 720, 900, and
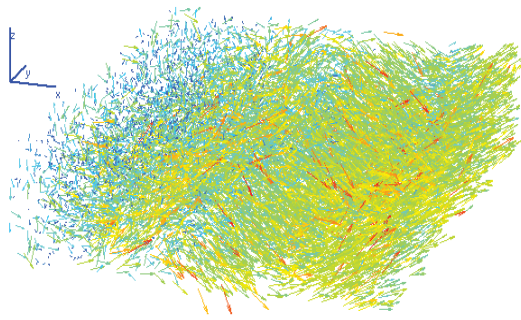
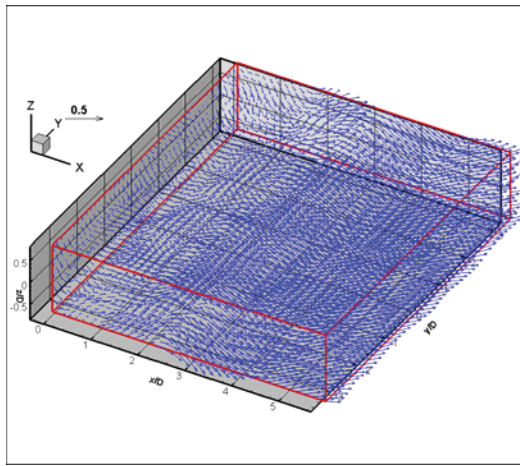Fig. 7 Instantaneous 3D vector field(Re=360).

Fig. 8 Instantaneous interpolated vectors (Re=360).

1080. With increase of Reynolds number, the maximum value of $|v'|/U_o$ increased, which implies that v' component (spanwise fluctuations) mainly contributes to the energy balancing of the turbulent structure at high Reynolds number. $|u'|/U_o$ value was maximum at Re=720. At low Reynolds numbers, v' component showed B-mode structure while u' component showed B-mode structure(Brede et al., 1996) at high Reynolds numbers. Regardless of Reynolds numbers, the distribution of the u' component showed a well organized structure near wake region, which implies that the energy cascade of the u' component occurs with regular patterns at near wake and irregular pattern at downstream.

SUMMARIES

Turbulent properties of a circular cylinder wake have been investigated by using a newly constructed Volume PTV. For successful measurements, a hybrid fitness function and a coherency fitness function have been adopted. More than 10,000 instantaneous 3D velocity vectors could be obtained by the constructed Volume PTV system. Obtained velocity vector fields showed reasonable physical properties on the circular cylinder wake.
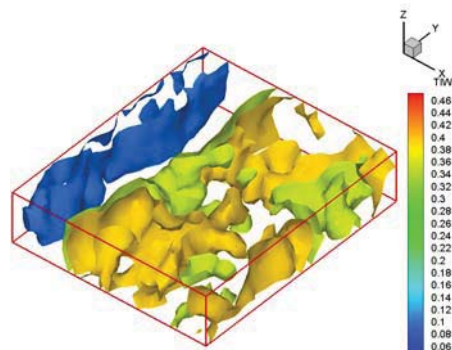
The optimal parameters used the measurements were PM[particle movements]= 8pixels, PN[particle neighborhood] =5mm and VF[vector fitness] =0.3.
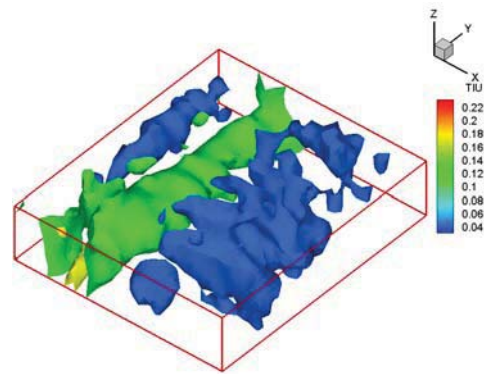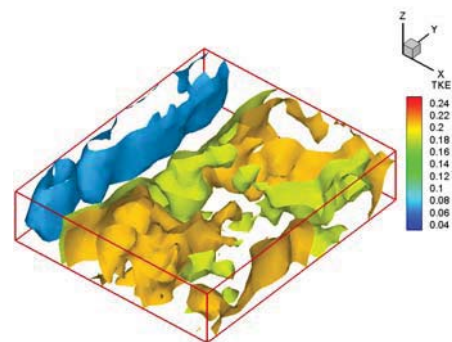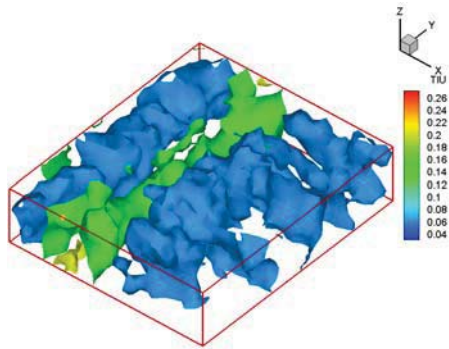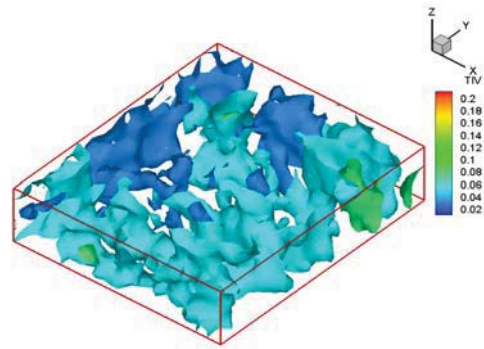

(a) $|u'|/U_o$
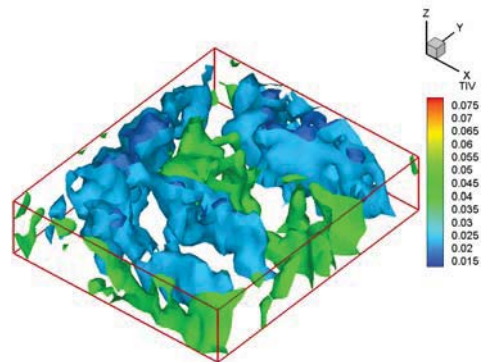
(b) $|v'|/U_o$
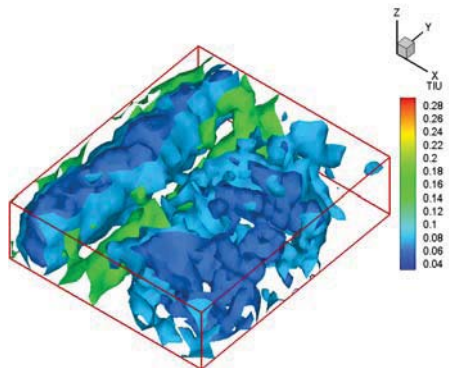

(c) $|w'|/U_o$

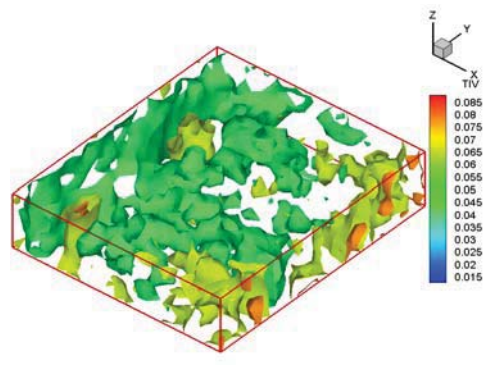(d) $\sqrt{u'^2+v'^2+w'^2}\,/U_o$
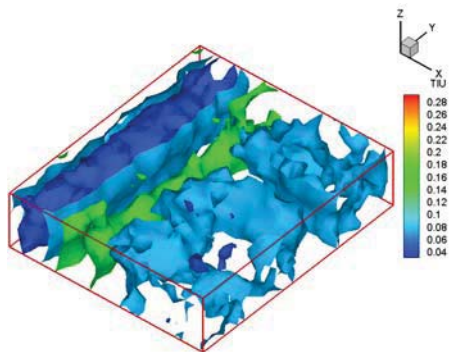
Fig. 9 Turbulence properties (Re=360).
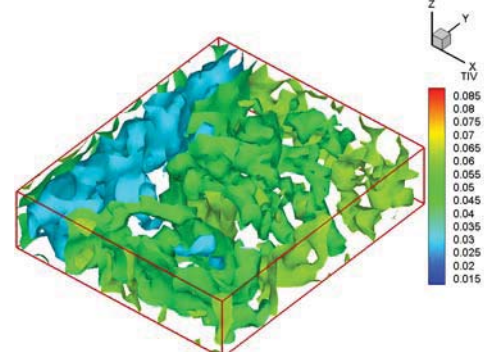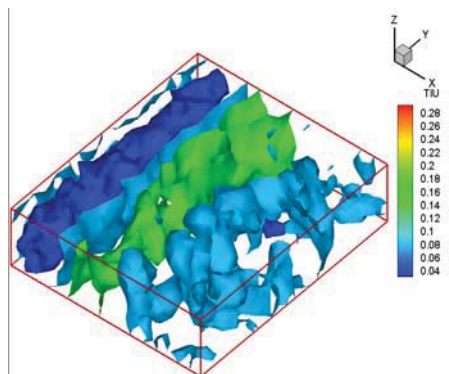
414

(a) at Re=540

(a) at Re=540
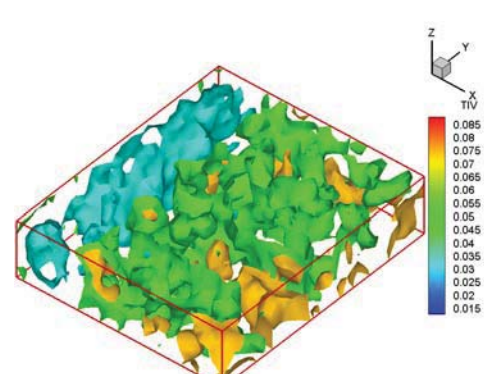
(b) at Re=720

(b) at Re=720

(c) at Re=900

(c) at Re=900

(d) at Re=1080

(d) at Re=1080

Fig. 10 Spatial distribution of $|u'|/U_o$.

Fig. 11 Spatial distribution of $|v'|/U_o$.

From the measurements, several outcomes are as follows.

For all Reynolds number cases, $\left|w'\right| > \left|u'\right| > \left|v'\right|$ was satisfied, and each value was 2 times higher than others. w' distribution has a strong relation with that of the turbulent kinetic energy $\sqrt{u'^2+v'^2+w'^2}/U_o$, which implies that w' component largely influences the turbulent properties of the wake.

From the analyses on the vertical structure, it showed that the distance between the second primary vortex and the third primary vortex was 1.5 times longer than that of the distance between the first primary vortex and the second primary vortex.

ACKNOWLEDGEMENTS

REFERENCES

Arroyo, M. P., and Greated, C. A., 1991, "Stereoscopic Particle Image Velocimetry", *Meas. Sci Technol*, Vol 2, pp. 1181-1186.

Brede, M., Eckelmann, H., and Rockwell, D., 1996, "On Secondary Vortices in the Cylinder Wake", *Phys. Fluids*, Vol. 8, pp. 2117-2124.

Chan, VSS., Koek, WD., Barnhart, D.H., Bhattacharya, N., Braat, JJM. & Westerweel, J. 2004. "Application of Holography to Fluid Flow Measurements using Bacteriorhodopsin", *Meas Sci Technol*, Vol 15, pp. 647-655.

Coëtmellec, S., Buraga-Lefebvre, C., Lebrun, D., and Özkul, C. 2001, "Application of In-line Digital Holography to Multiple Plane Velocimetry", *Meas Sci Technol*, Vol 12, pp.1392-1397.

Doh, D. H., Hwang, T. G., and Saga, T., 2004, "3D-PTV Measurements of the Wake of a Sphere", *Meas Sci Technol*, Vol.15, No. 6, pp.1059 - 1066.

Doh, D.H., Kim, D.H., Cho, K.R., Cho, Y.B., Saga, T., and Kobayashi, T. 2002, "Development of Genetic Algorithm based 3D-PTV Technique", *Journal of Visualization*, Vol. 5, No.3, pp.243-254.

Hinsch, K. D., 2002, "Holographic Particle Image Velocimetry", *Meas Sci Technol*, Vol 13, pp. R61-R72.

Kähler, C. J., and Kompenhans, J., 2000, "Fundamentals of Multiple Plane Stereo Particle Image Velocimetry", *Exp Fluids, Supp*l, pp. S70-S77.

Kim, S., and Lee, S.J., 2008 "Effect of Particle Number Density in In-line Digital Holographic Particle Velocimetry", *Exp. in Fluids*, Vol.44. pp.623-631.

Monkewitz, P.A., 1988. "The Absolute and Convective Nature of Instability in Two-Dimensional Wakes at Low Reynolds Numbers", *Phys. Fluids*, Vol. 31, pp. 999–1006.

Scarano, F., Elsinga, G.E., Bocci, E, and van Oudheusden, B.W. 2006 "Investigation of 3-D Coherent Structures in the Turbulent Cylinder Wake using Tomo-PIV", *CD-ROM Proc. of 13th Intl' Symp. on Appl. of Laser Tech. to Fluid Mech.*, Lisbon, 26-29 June.

Sung J., and Yoo, J. Y., 2001, "Three-Dimensional Phase-Averaging of Time-Resolved PIV Measurement Data", *Meas. Sci. Technol.*, Vol. 12, pp. 655-662.

Thompson, M., Hourigan, M., and Sheridan, J., 1996. "Three Dimensional Instabilities in the Wake of a Circular Cylinder", *Exp. Therm. Fluid Sci.*, Vol. 12, pp. 190–196.

Williamson, C.H.K., 1996a, "Vortex Dynamics in the Cylinder Wake", *Ann. Rev. Fluid Mech.*, Vol. 28, pp. 477–539.

Williamson, C.H.K., 1996b, "Three Dimensional Wake Transition", *J. Fluid Mech.*, Vol. 328, pp. 345–407.